Data of Model Experiments for Ship A-2

prepared by N. Umeda in March 2000

1. Details of Ship A-2

Free-running model experiments were carries out with a 1/15 scaled model of a 135 gross tonnes purse seiner of which principal particulars are shown in Table 1 and the body plan is presented in Fig. 1. The offset data file, seiner.off, is also provided as a form of text file in full scale. The righting arm curves in calm water with the metacentric height of 1.00 m are shown in Fig.2. This ship critically complies with the IMO intact stability code. The model is fitted with forecastle and bilge keels. Deck houses were not realised on the model because stability criteria ignore them as non-watertight structures. To store experimental equipment, additional watertight hatches and their coamings were fitted on the upper deck. The details of the layout of upper deck is given in Fig. 3. Inside the model hull, a DC motor for propulsion, a steering gear, gyroscope, batteries and on-board computer were equipped. By using the on-board computer, the auto pilot is simulated and the propeller revolution is controlled to be constant. During the experiments, the ship model is self-propelled and is completely free. The propeller thrust coefficient obtained by the propeller open test is given in Fig. 4. The thrust deduction fraction obtained by the self-propulsion test is 0.142.

2. Data of the capsizing model experiments

This series of model experiments were carried out at the seakeeping and manoeuvring basin of National Research Institute of Fisheries Engineering (NRIFE). The details of these experiments were reported in Umeda et al. (1999). The ship model ran to keep a straight course by using the auto pilot in regular following and quartering waves. Among many model runs, 4 model runs are selected for the ITTC benchmark testing. The control parameters for these selected runs are shown in Table 2. Until a generated wave train propagated enough, the model was kept near the wave maker without propeller revolution. Then the model started to drift and, at a certain moment, we commanded the propeller revolution to immediately increase up to the specified one and auto pilot to be active for the specified course. At this moment, the on-board computer started to measure and store the data. Thus, these first data can be regarded as the initial conditions for numerical simulation, which is provided in Table 3. The measure time histories are shown in Figs. 5-8 in model scale. The measured items consist of the pitch angle, the pitch rate, the roll angle, the roll rate, the yaw angle, the yaw rate, the surge acceleration, the sway acceleration, the heave acceleration, the rudder angle and the propeller revolution number. The data files, specified in Table 2, involve digital values of the pitch, roll, yaw and rudder angle as well as the propeller revolution number as functions of time in model scale. The roll decay test was carried out without a forward velocity and its result is shown in Figs. 9-10.

3. Data of manoeuvring model test

The free-running model test was also carried out at the seakeeping and manoeuvring basin of NRIFE. The control and measuring system is as same as that used for the capsizing model experiments but with new algorithm for manoeuvring tests. Fig. 11 shows the time history of -35 degrees turning manoeuvre at the Froude number of 0.3. Those consist of the rudder, roll and yaw angles.

4. Data of captive model tests

For estimating hydrodynamic coefficients, several captive tests were carried out at the seakeeping and manoeuvring basin of National Research Institute of Fisheries Engineering (NRIFE). The results of the resistance test and the heel angle tests are shown in Fig. 12 and 13, respectively. The rudder angle test results are shown in with several identified coefficients in Figs. 14-16. The results of circular motion tests (CMT) are shown in Figs. 17-18. Here the surge force, X, sway force, Y, the yaw moment, N and the are plotted as functions of the the drift angle, β, and the non-dimensional yaw rate, r’. The mathematical model on the derivatives of hydrodynamic lateral force and yaw moment in calm water with respect to the rudder angle is based on the MMG model (Ogawa and Kasai, 1978) and is given as follows:

$$Y_\delta = -(1+a_H)\frac{1}{2}\rho A_R U_R^2 f_\alpha \alpha_R$$
$$N_\delta = -(x_R + a_H x_H)\frac{1}{2}\rho A_R U_R^2 f_\alpha \alpha_R$$

where

$$U_R = \sqrt{u_R^2 + v_R^2}$$
$$\alpha_R = \delta - \tan^{-1}(v_R / u_R)$$
$$f_R = \frac{6.13\Lambda}{2.25+\Lambda}$$
$$u_R = \varepsilon_R (1-w_p) U \sqrt{1+\kappa_p \frac{8K_T}{\pi J^2}}$$
$$v_R = v_{RP} - \gamma_R (v + l_R r)$$
$$J = \frac{(1-w_P)U}{nD_P}$$

5. Example of benchmark testing

As an example, the benchmark test results executed by Osaka University are shown in Figs. 19-22. These are the comparison between the capsizing model test results and results with Osaka University's numerical code for the ship A-2. Here the pitch angle, θ, the roll angle, φ, the heading angle, χ, the rudder angle, δ, are presented. The details of this numerical method are described in Umeda (1999).

References

Ogawa, A. and Kasai, H. (1978) On the Mathematical Model of Manoeuvring Motion, International Shipbuilding Progress, 25:306-319.

Umeda, N. et al. (1999) Stability Assessment for Intact Ships in the Light of Model Experiments, Journal of Marine Science and Technology, 4:45-57.

Umeda, N. (1999) Nonlinear Dynamics of Ship Capsizing due to Broaching in Following / Quartering Seas, Journal of Marine Science and Technology, 4:16-26.

Nomenclatures

a_H	:	interaction factors
A_R	:	rudder area

f_α : lift coefficient of rudder alone

K_T : thrust coefficient of propeller

l_R : correction factor for flow-straightening effect due to yaw rate

n : propeller revolution number

r : yaw rate

U_R : effective rudder inflow velocity

u_R : component of effective rudder inflow velocity in x direction

v_R : component of effective rudder inflow velocity in y direction

v_{RP} : effective rudder inflow velocity due to unsymmetric rotation of propeller

w_P : effective propeller wake fraction

α_R : effective rudder inflow angle

β : drift angle (=-sin-1(v/U))

γ_R : flow-straightening effect coefficient

δ : rudder angle

ε : wake ratio between propeller and rudder

κ_P : interaction factor between propeller and rudder

Λ : rudder aspect ratio

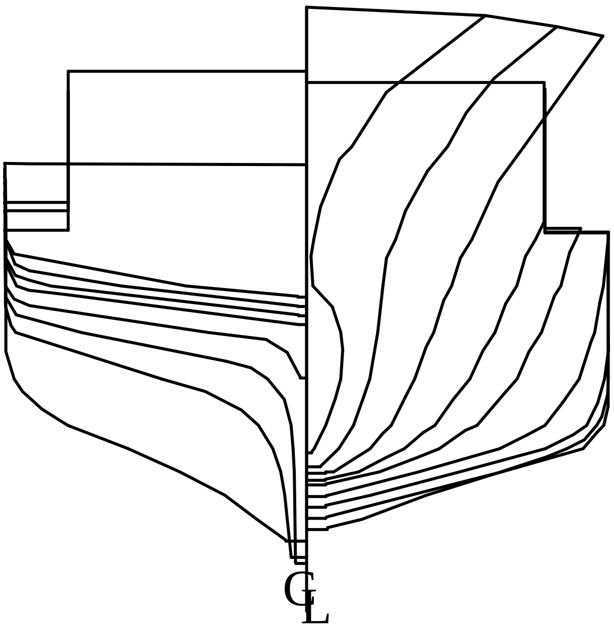

Fig. 1 Body plan of Ship A-2

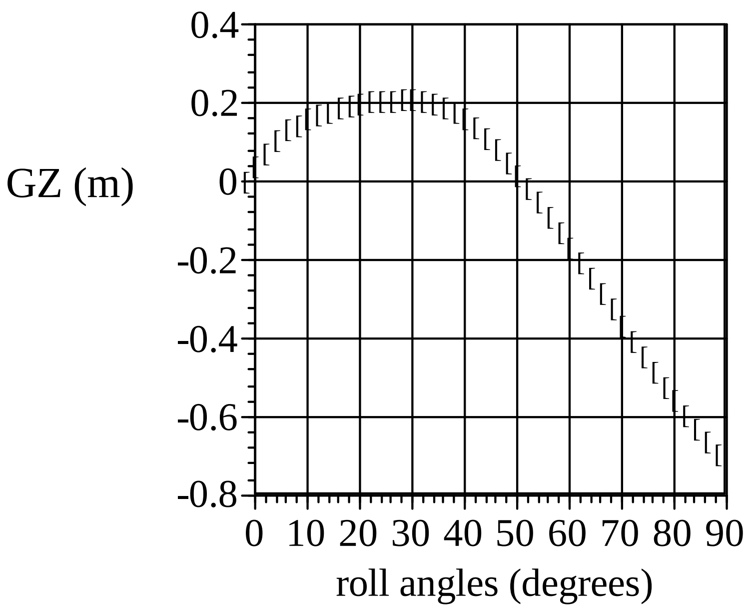

Fig. 2 Calculated righting arm curve of Ship A-2 in calm water in full scale

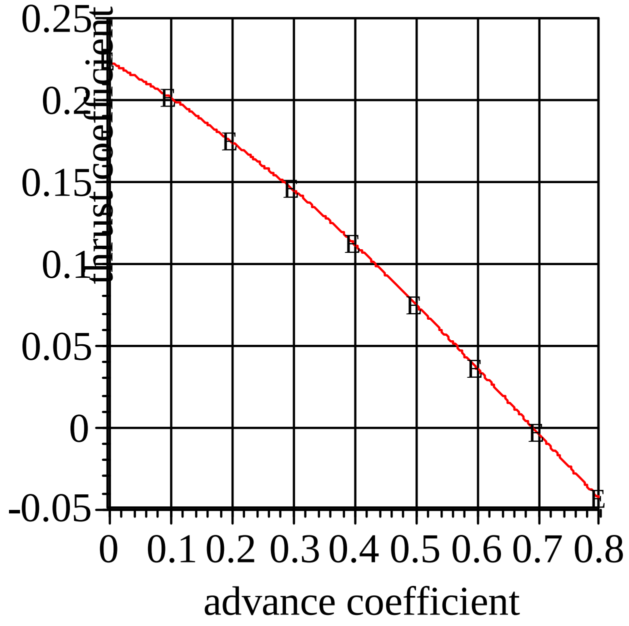

Fig. 4 Propeller thrust coefficient obtained from the propeller open test

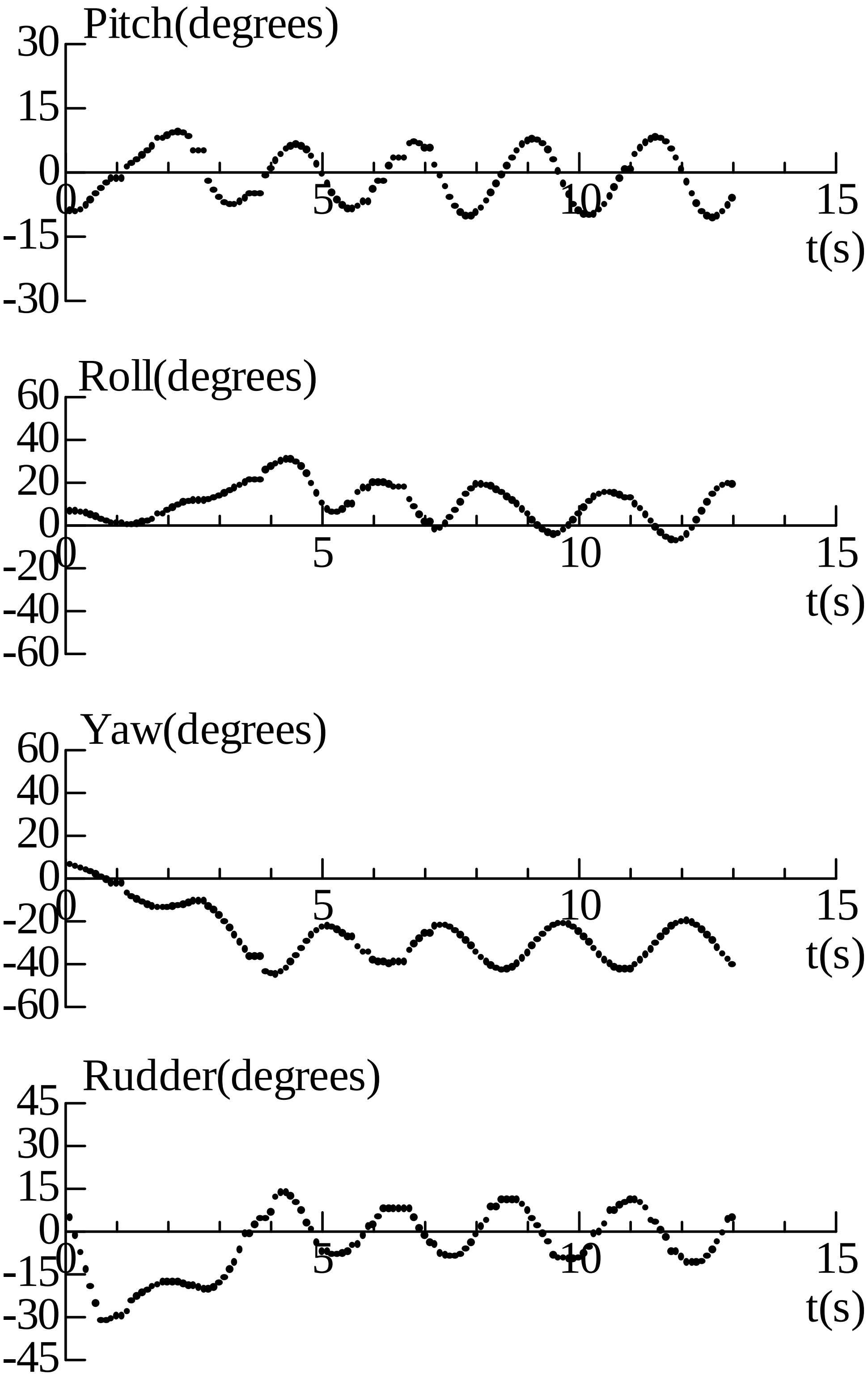

Fig. 5 Measured time history of the free-running model run of the ship A-2 in model scale with H/λ=1/10.0, λ/L=1.637,F_n=0.3 and χ_C=-30.0 °

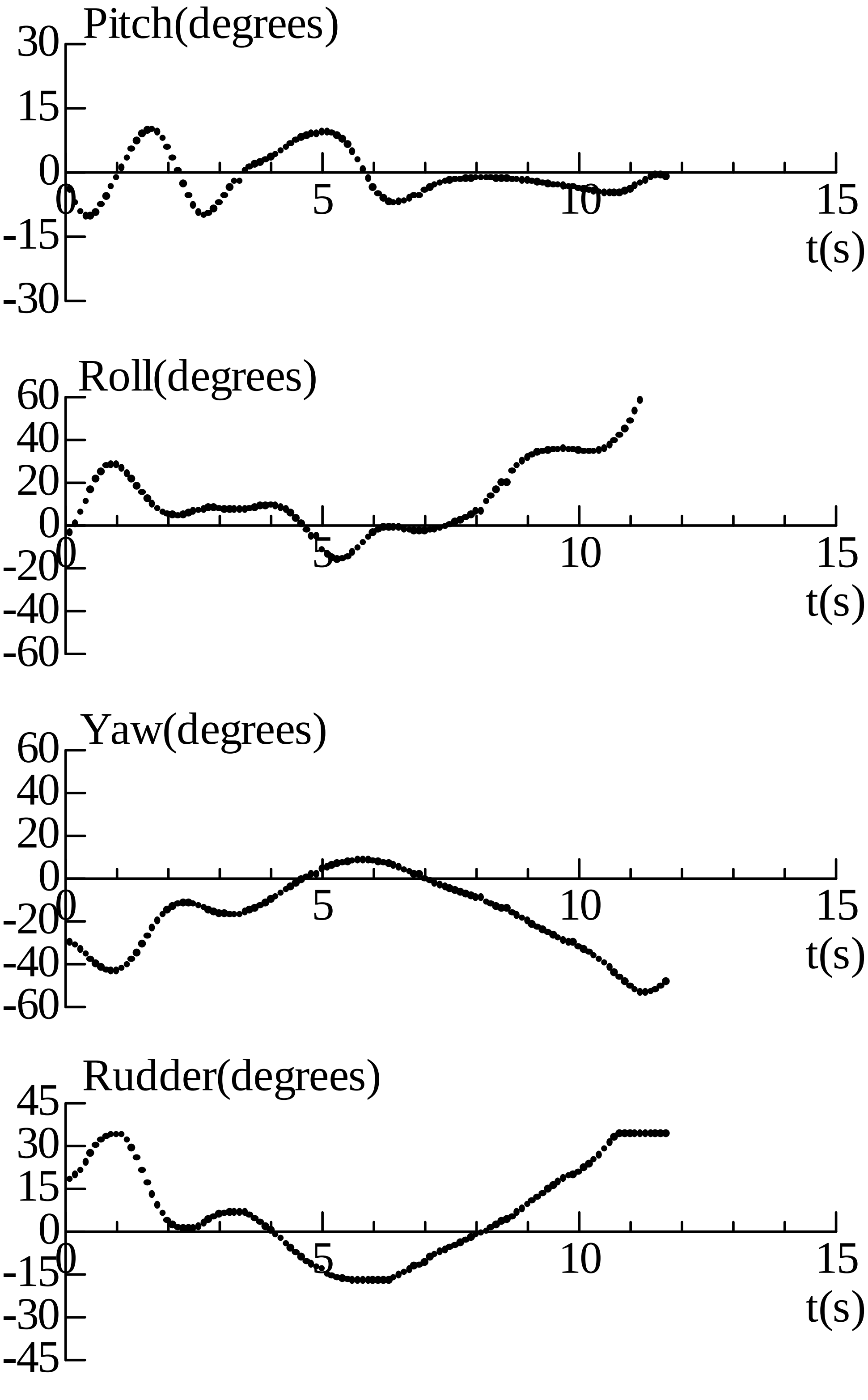

Fig. 6 Measured time history of the free-running model run of the shipA-2 in model scale with H/λ=1/10.0, λ/L=1.637,F_n=0.43 and χ_C=-10.0 °

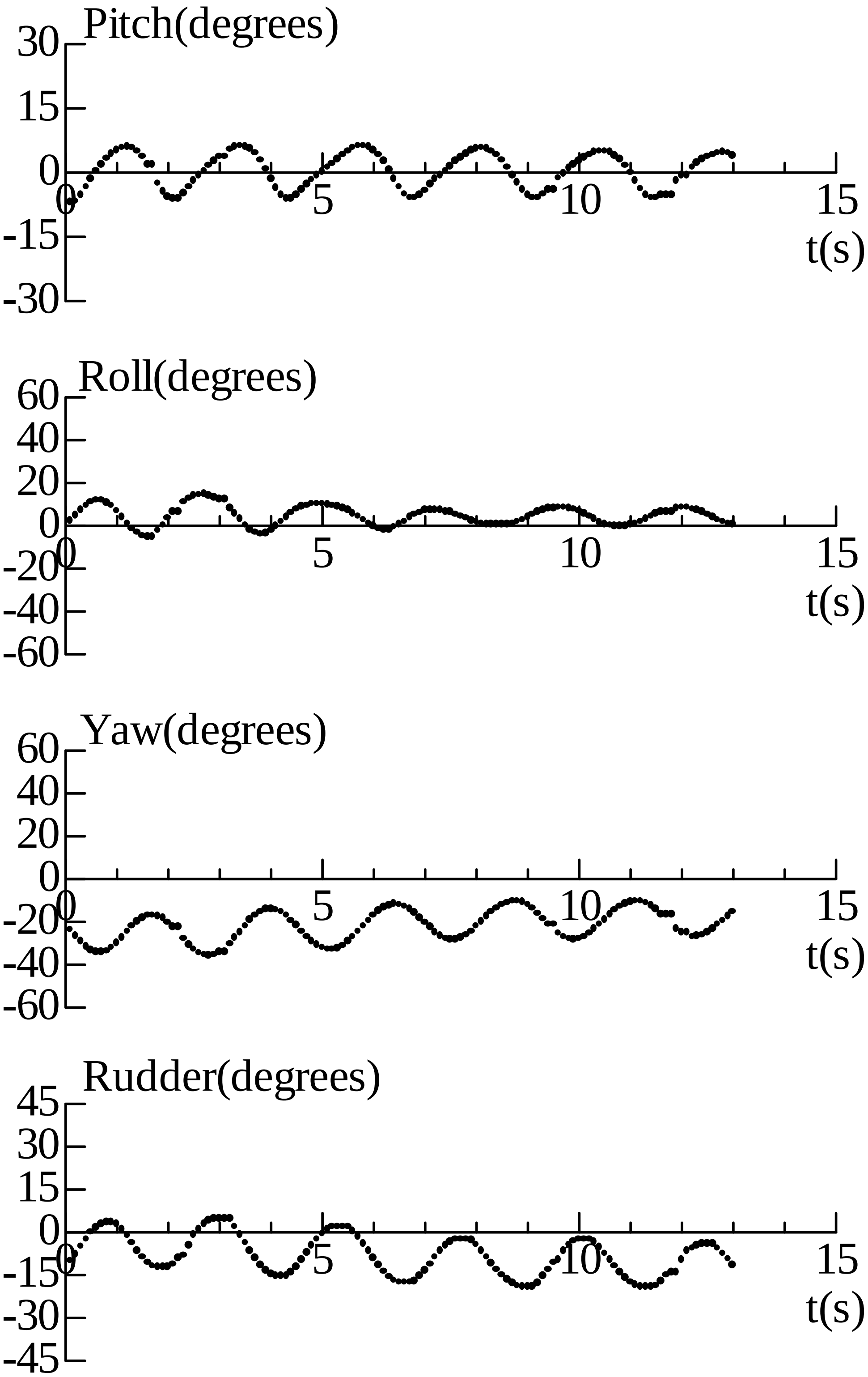

Fig. 7 Measured time history of the free-running model run of the ship A-2 in model scale with H/λ=1/8.7, λ/L=1.127,F_n=0.3 and χ_C=-30.0 °

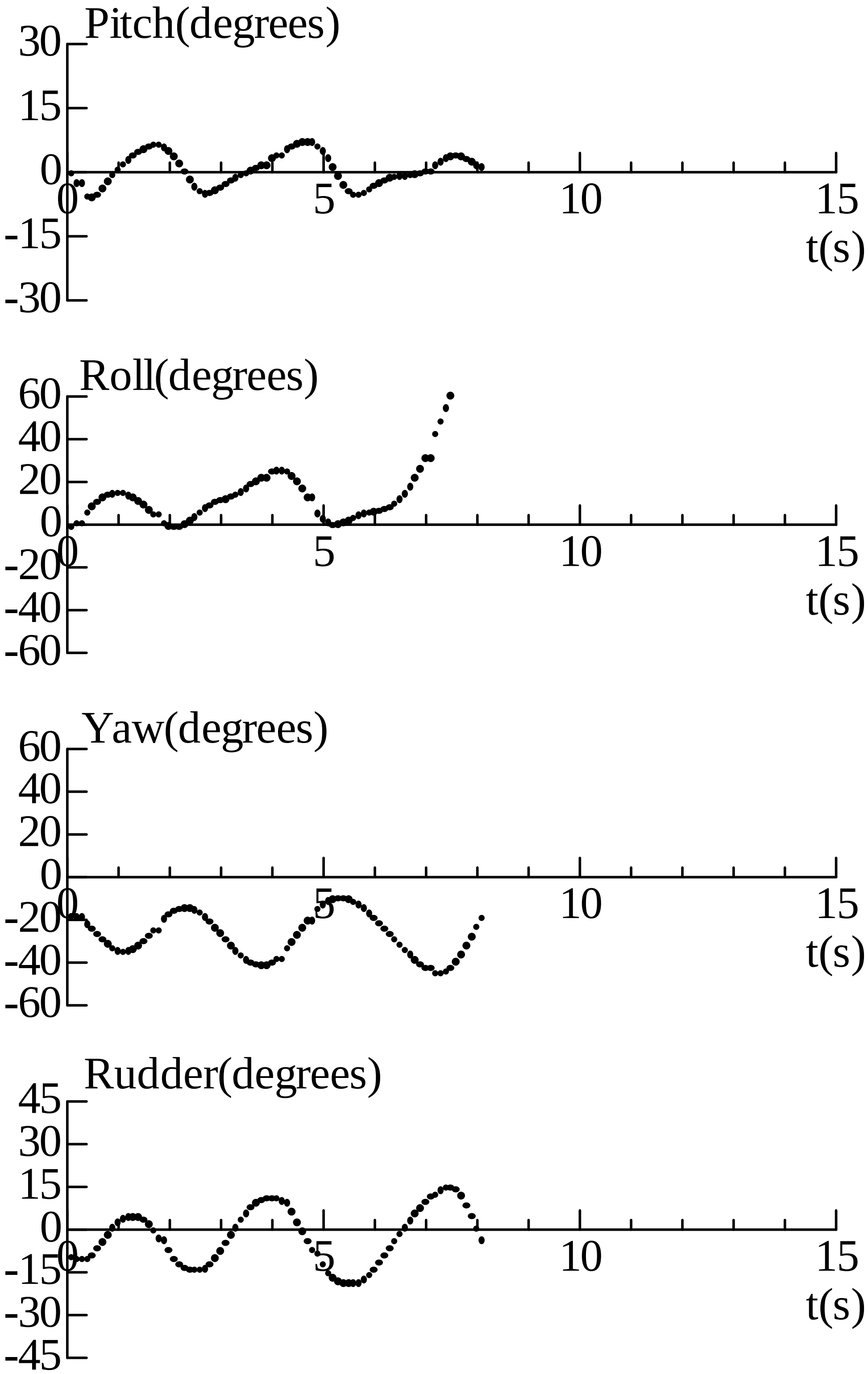

Fig. 8 Measured time history of the free-running model run of the ship A-2 in model scale with H/λ=1/8.7, λ/L=1.127,F_n=0.43 and χ_C=-30.0 °

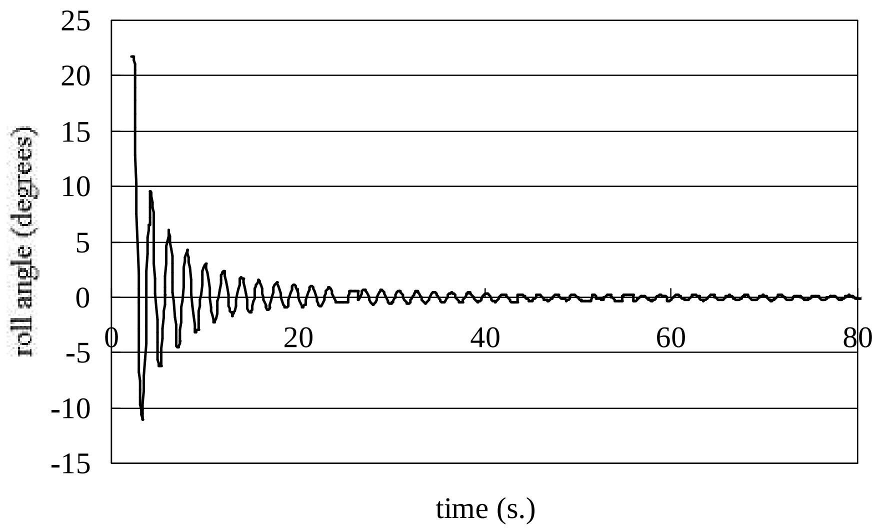

Fig. 9 Measured time history of the roll decay test of the ship A-2 without forward velocity in model scale

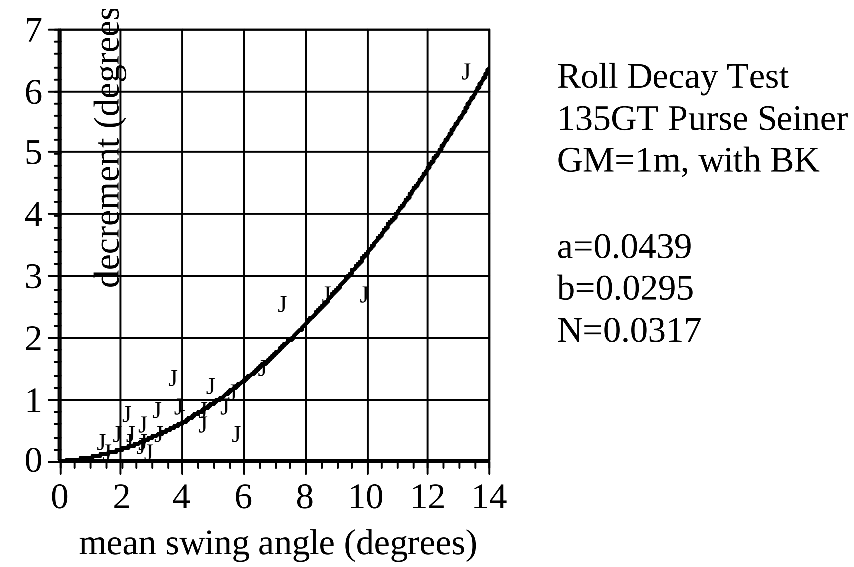

Fig. 10 Extinction curve from the roll decay test data such as Fig. 9. As indicated by a solid line, the relationship between the decrement, $\Delta\phi$, and the mean swing angle, ϕ_m, is fitted with the following formula: $\Delta\phi_m = a\phi_m + b\phi_m{}^2$

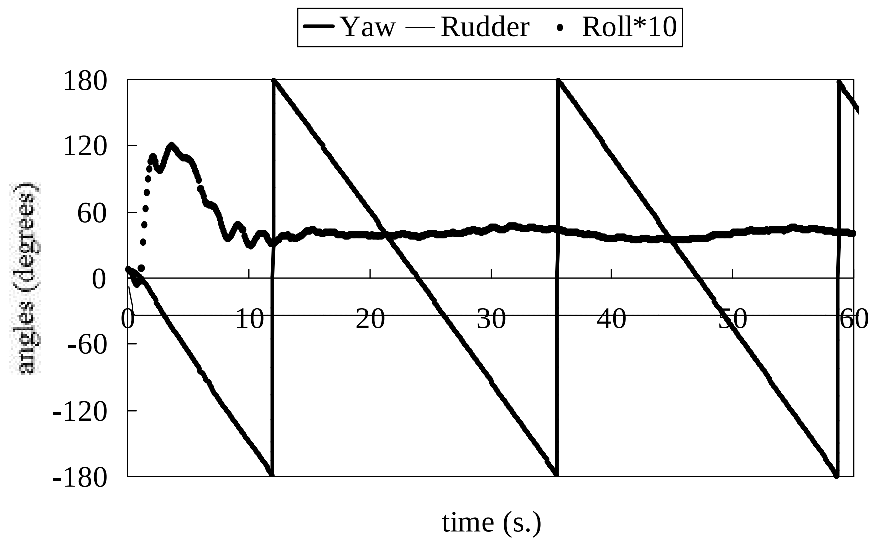

Fig. 11 Measured time histories of the –35 degrees turning test of Ship A-2 at Fn=0.30 in model scale

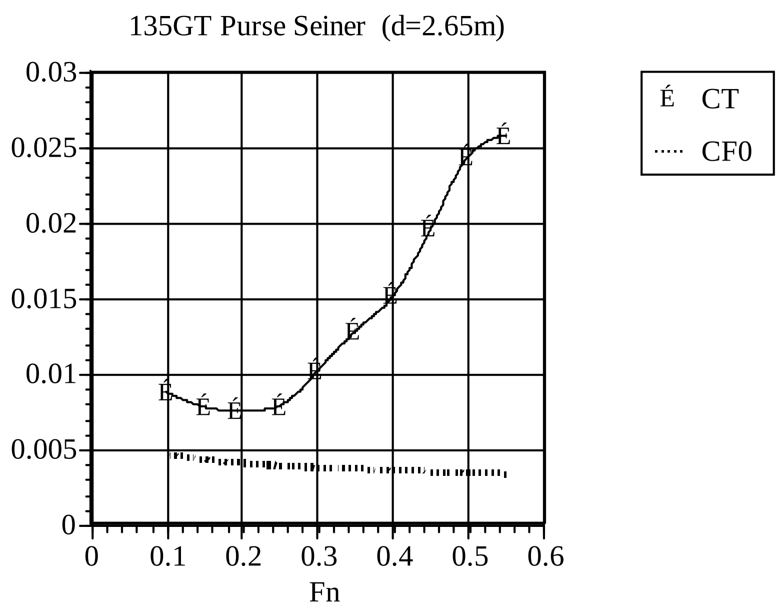

Fig. 12 Resistance coefficient from the resistance test for Ship A-2

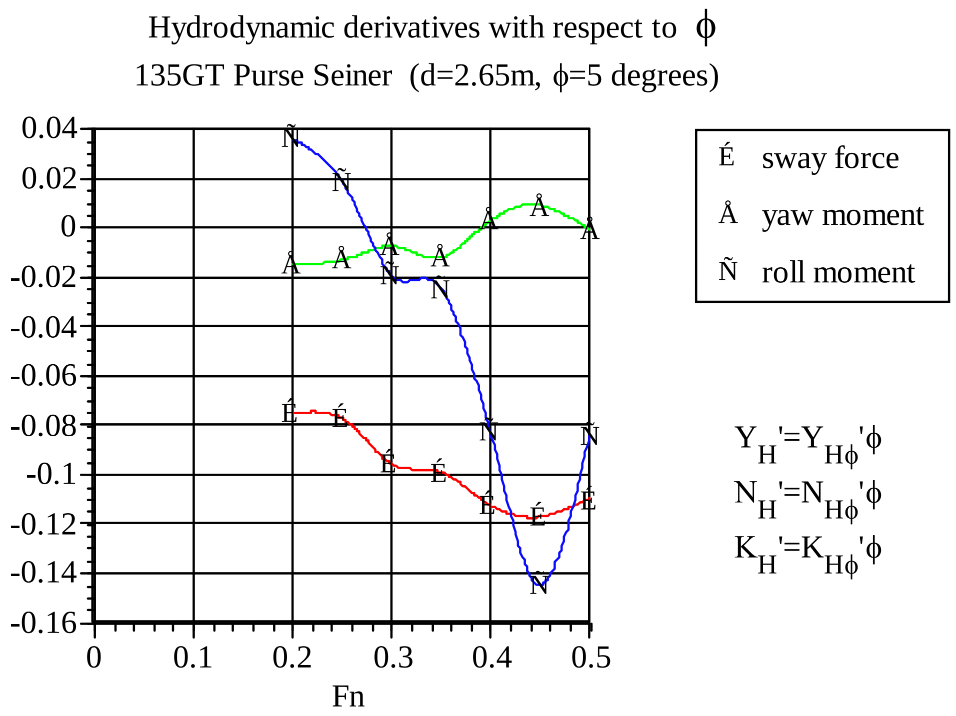

Fig. 13 Non-dimensional derivatives of hydrodynamic forces with respect of heel obtained from the heel angle tests for Ship A-2

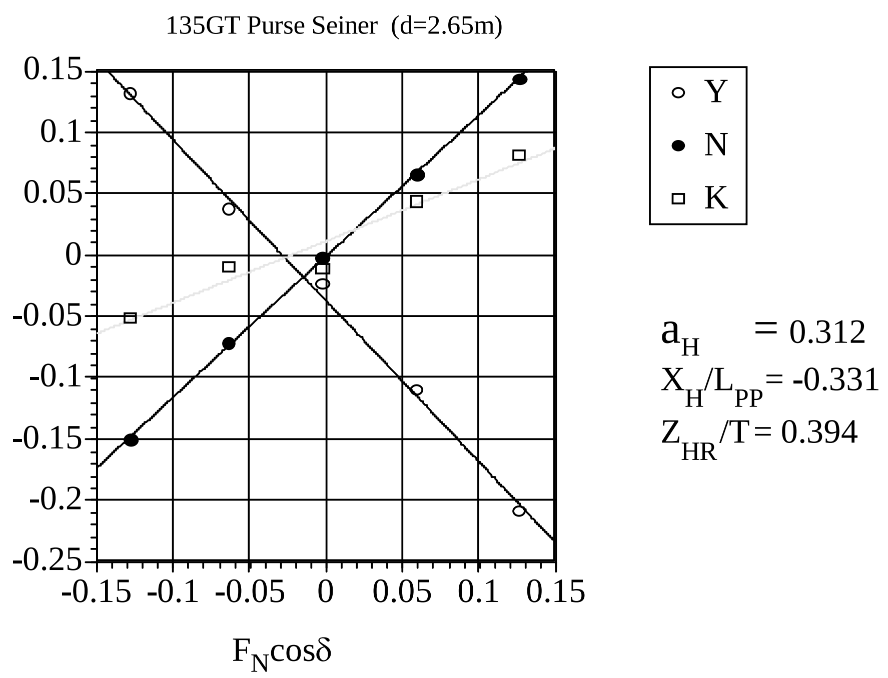

Fig. 14 Interaction between hull and rudder obtained from the Rudder angle test results of Ship A-2 at Fn=0.2

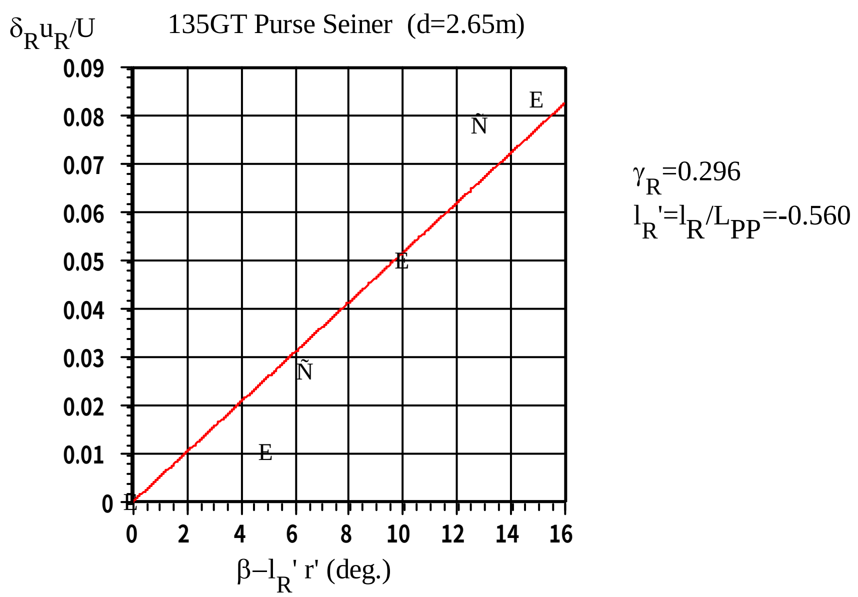

Fig. 15 Flow-straightening effect obtained by the circular motion test with rudder angle for Ship A-2 at Fn=0.2.

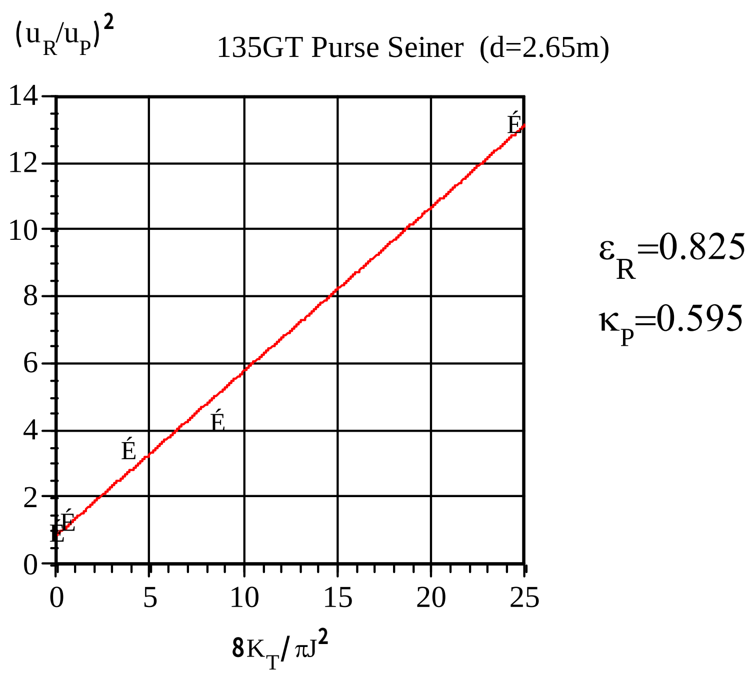

Fig. 16 Interaction between propeller and rudder obtained by the rudder angle tests for Ship A-2 at Fn=0.2

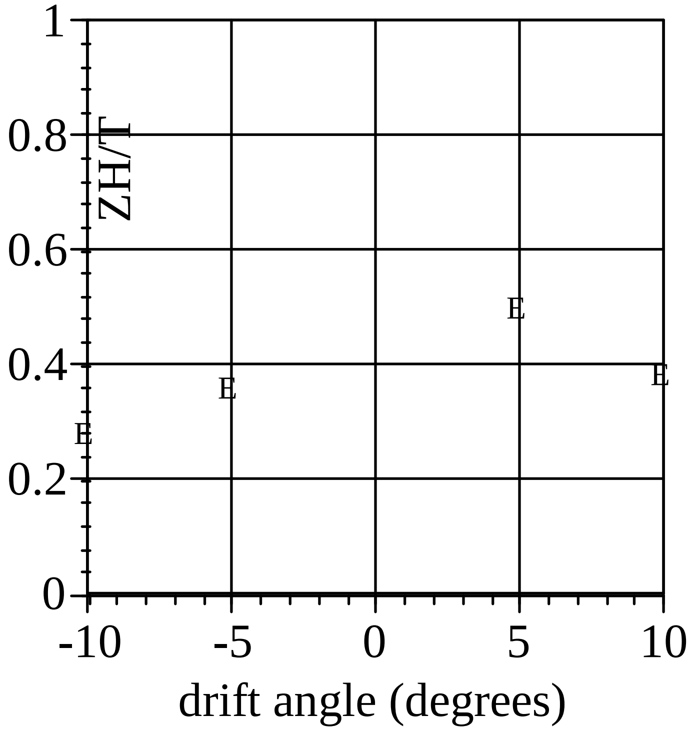

Fig. 18 Vertical distance of the centre of lateral force from the water surface obtained from the oblique towing tests for the ship A-2 at Fn=0.2

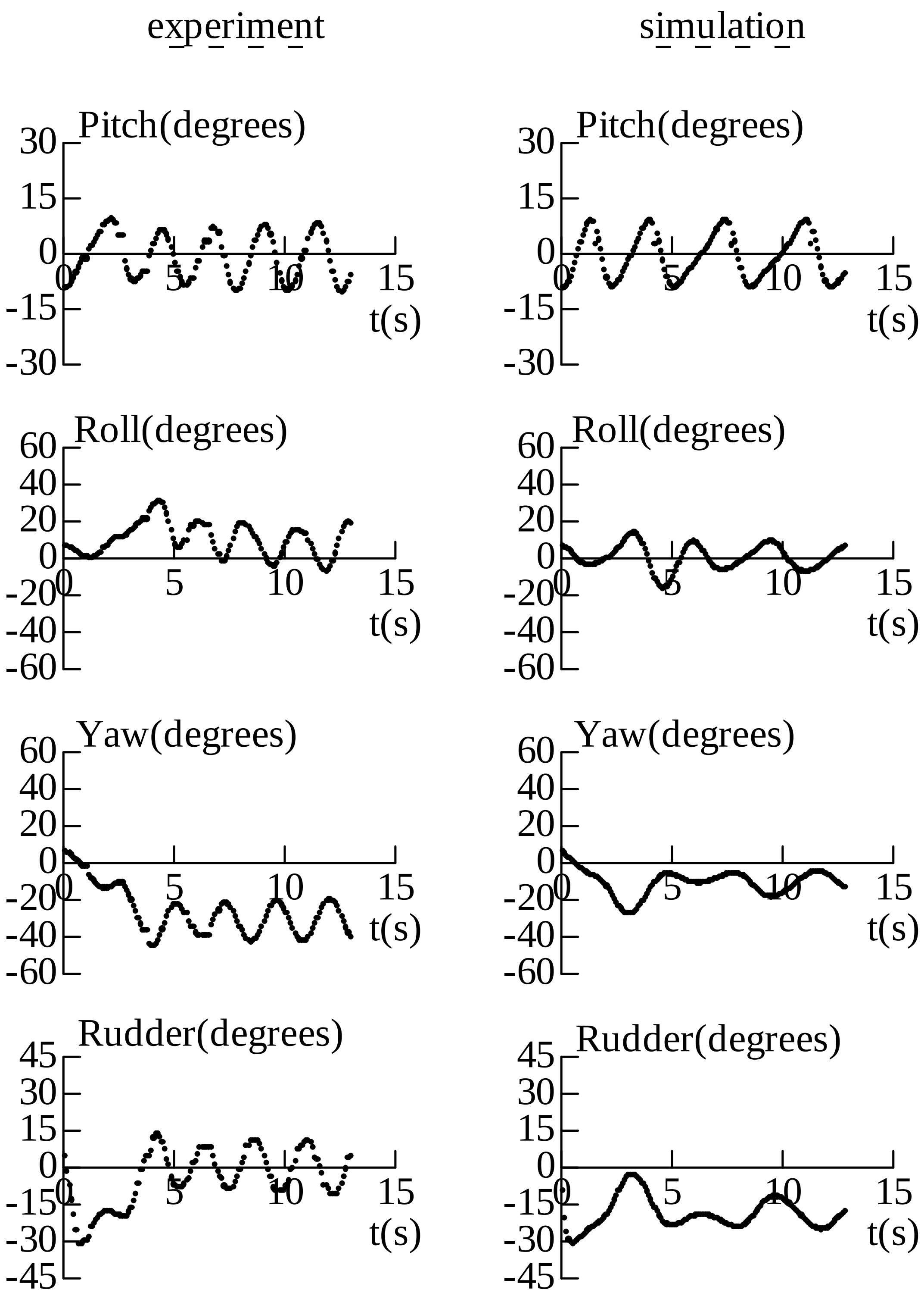

Fig. 19 Comparison between the experiment and the numerical code of Osaka University (Umeda,1999) for the shipA-2 in model scale with H/λ=1/10.0, λ/L=1.637, F_n=0.3 and χ_C=-30.0°

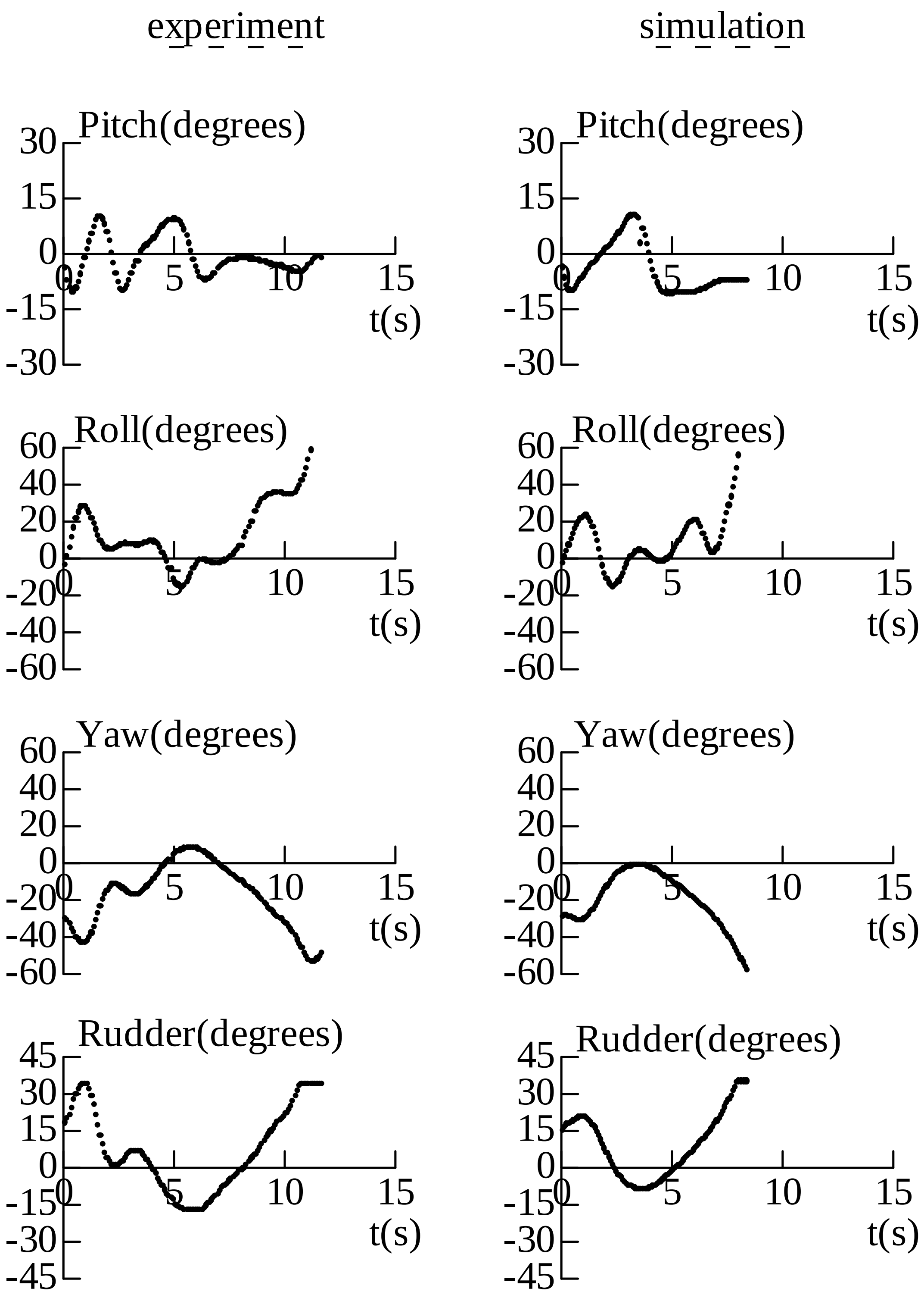

Fig. 20 Comparison between the experiment and the numerical code of Osaka University (Umeda,1999) for the shipA-2 in model scale with H/λ=1/10.0, λ/L=1.637,F_n=0.43 and χ_C=-10.0 °

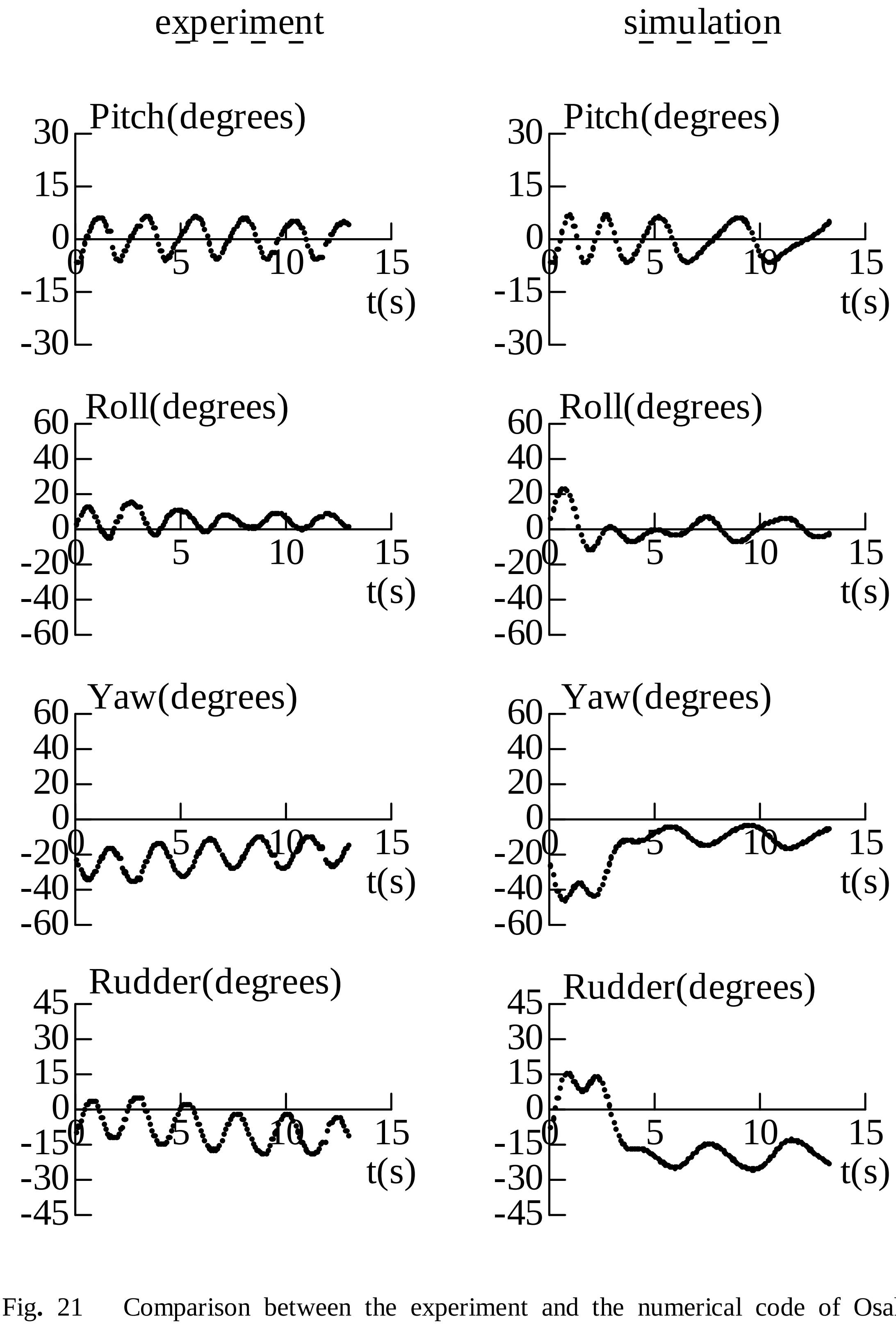

Fig. 21 Comparison between the experiment and the numerical code of Osaka University (Umeda,1999) for the shipA-2 in model scale with H/λ=1/8.7, λ/L=1.127,F_n=0.3 and χ_C=-30.0 °

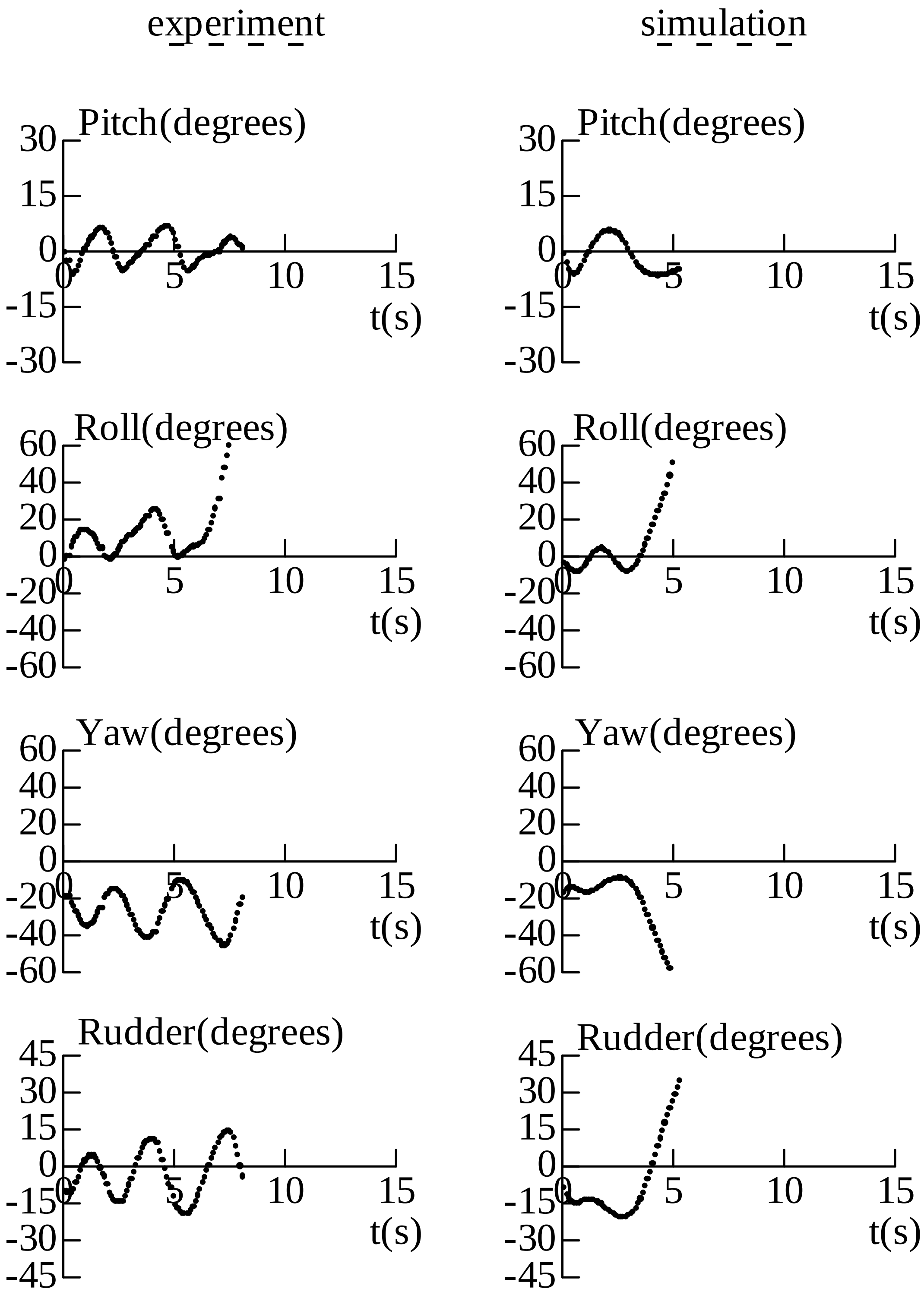

Fig. 22 Comparison between the experiment and the numerical code of Osaka University (Umeda,1999) for the shipA-2 in model scale with $H/\lambda=1/8.7$, $\lambda/L=1.127$, $F_n=0.43$ and $\chi_C=-30.0°$

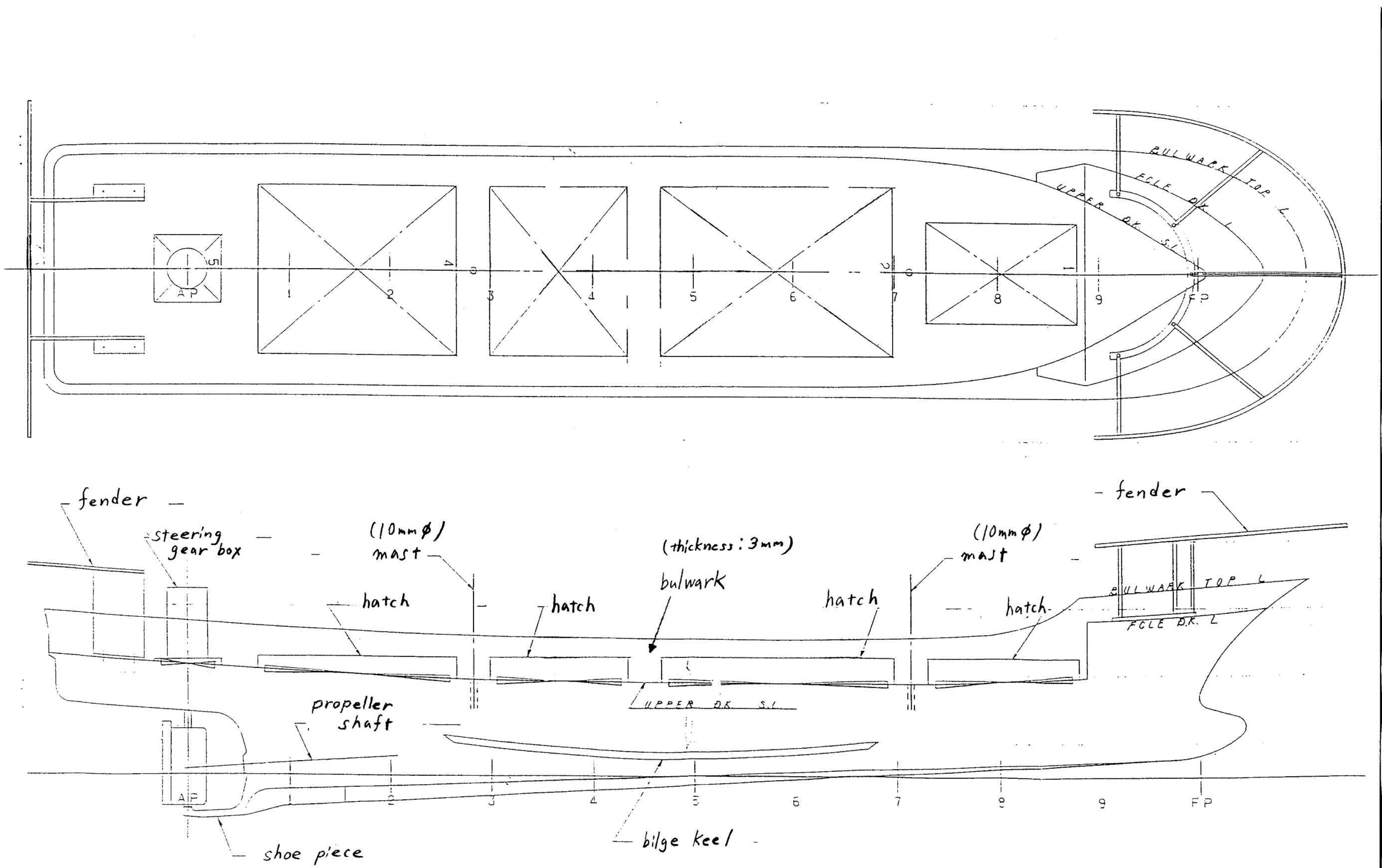

Fig. 3 layout of the superstructure of the model of ship A-2 in model scale

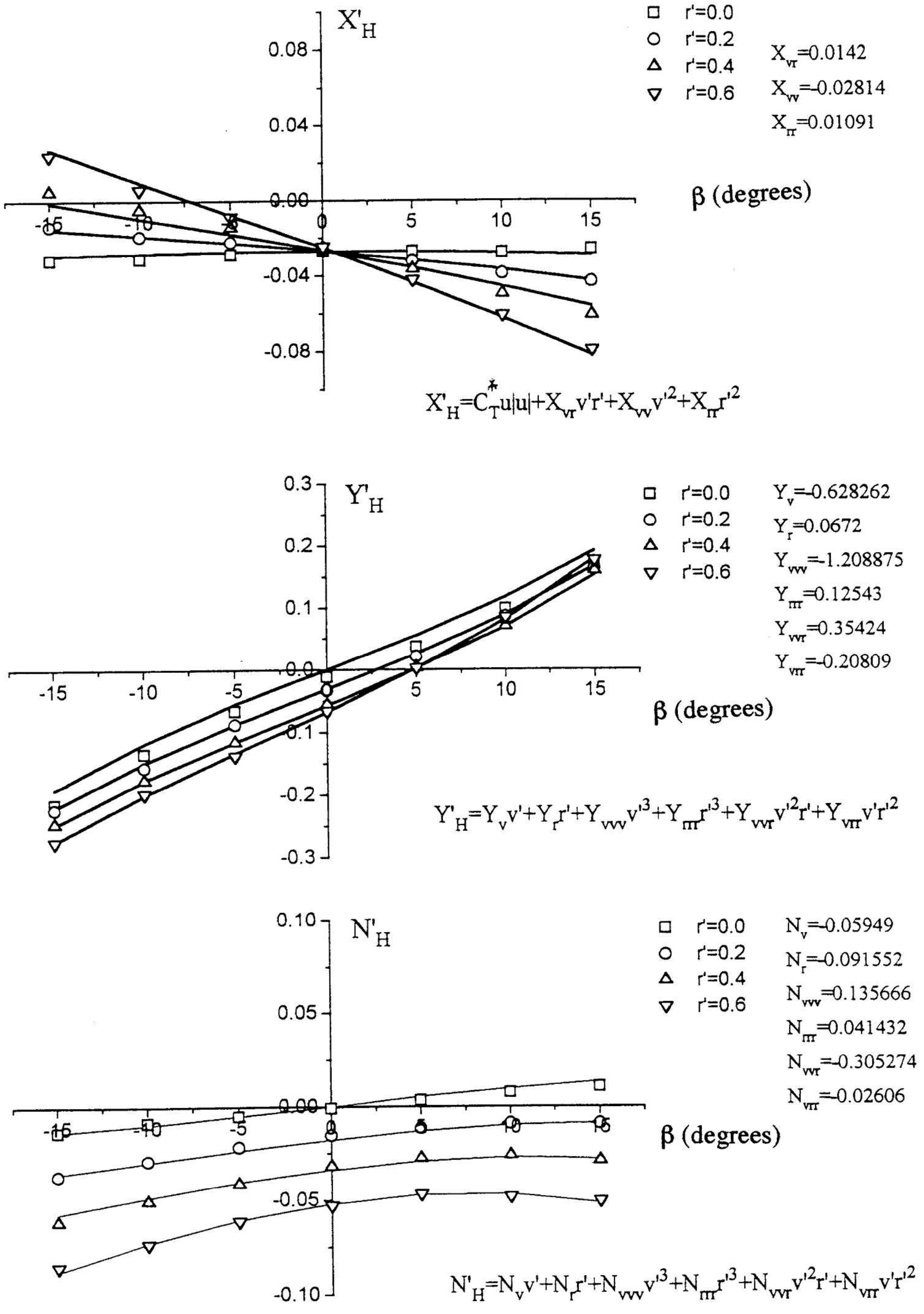

Fig. 17 Results of the circular motion tests of the ship A-2 at Fn=0.2.

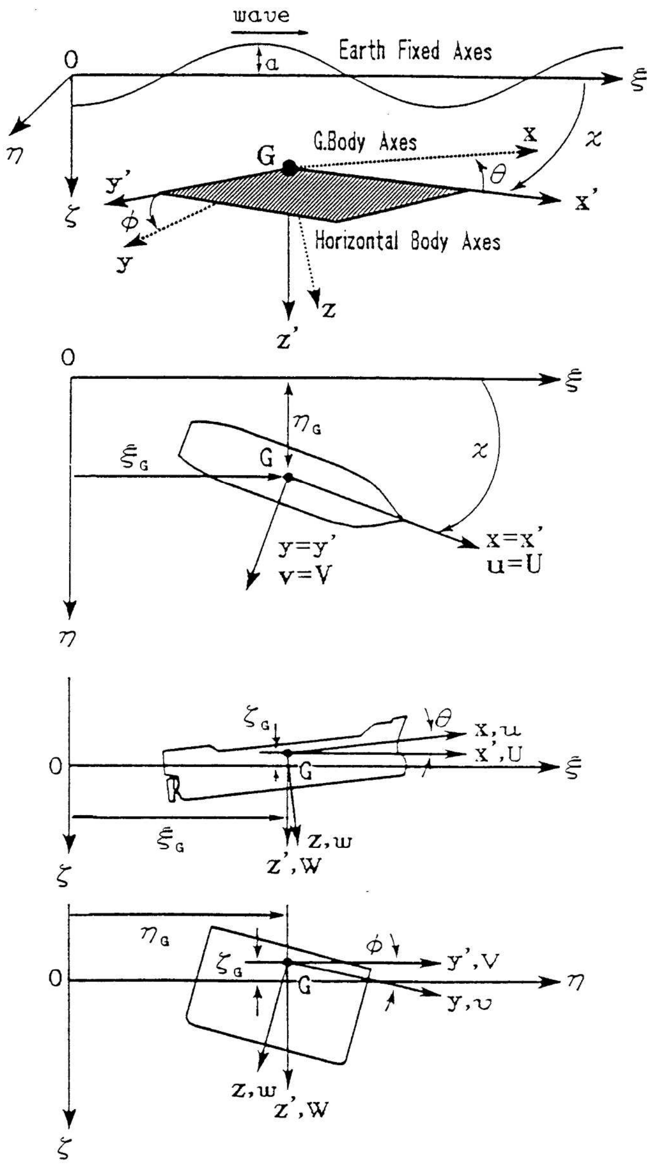

Fig. 23 Co-ordinate systems

```
Offset data of the purse seiner
prepared by Osaka University, Japan

19 / number of transverse sections
(D section)
4,-21.65        /number of sample points at this section, position of this section
in x
 0.000,3.800    /sample points (y & z)
 0.000,3.805
 3.480,3.815
 3.800,3.820
(C section)
8,-20.55
 0.000,2.380
 0.110,2.380
 0.110,2.390
 1.515,2.500
 3.680,2.845
 3.785,3.000
 3.795,3.800
 3.800,3.820
(B section)
8,-.19.45
 0.000,2.280
 0.110,2.280
 0.110,2.285
 2.330,2.500
 3.490,2.665
 3.670,2.735
 3.790,3.000
 3.800,3.760
(A section)
10,-.18.35
```

```
 0.000,2.180
 0.100,2.180
 0.100,2.190
 3.220,2.500
 3.500,2.565
 3.665,2.615
 3.785,2.800
 3.785,3.000
 3.790,3.640
 3.800,3.680
(AP section)
9,-.17.25
 0.000,2.085
 0.100,2.085
 3.000,2.405
 3.495,2.455
 3.650,2.500
 3.785,2.740
 3.785,3.000
 3.790,3.535
 3.800,3.610
(1/2 section)
12,-.15.53
 0.000,1.510
 0.080,1.510
 0.080,1.520
 0.245,1.785
 0.510,1.925
 1.235,2.000
 3.490,2.290
 3.680,2.360
 3.790,2.500
 3.795,3.000
```

3.795,3.370
3.800,3.510
(1 section)
20,-.13.80
0.000,-.485
0.135,-.485
0.140,-.470
0.150,0.250
0.155,0.500
0.170,0.750
0.195,1.000
0.280,1.280
0.490,1.500
0.700,1.620
1.010,1.690
2.835,2.000
3.655,2.190
3.785,2.380
3.790,2.500
3.790,3.000
3.790,3.310
3.800,3.400
3.000,3.400
3.000,4.600
(1+1/2 section)
20,-12.075
0.000,-.420
0.195,-.420
0.195,-.410
0.275,0.250
0.325,0.500
0.425,0.750
0.605,1.000

0.820,1.165
1.275,1.365
1.825,1.500
3.495,1.955
3.660,2.000
3.720,2.075
3.790,2.285
3.790,2.500
3.795,3.000
3.795,3.265
3.800,3.310
3.000,3.310
3.000,4.810
(2 section)
20,-.10.35
0.000,-.365
0.260,-.365
0.260,-.360
0.365,0.000
0.475,0.250
0.640,0.500
0.895,0.750
1.340,1.000
2.010,1.230
2.855,1.500
3.495,1.760
3.690,1.860
3.785,2.000
3.790,2.070
3.790,2.500
3.790,3.000
3.790,3.185
3.800,3.220

3.000,3.220
3.000,4.720
(3 section)
19,-.6.90
0.000,-.245
0.260,-.245
0.260,-.235
0.625,-.010
1.030,0.250
1.595,0.500
2.245,0.750
3.005,1.000
3.330,1.175
3.575,1.365
3.680,1.500
3.785,1.795
3.785,2.000
3.785,2.500
3.785,3.000
3.790,3.065
3.800,3.100
3.000,3.100
3.000,4.600
(4 section)
20,-.3.45
0.000,-.120
0.260,-.120
0.265,-.100
0.695,-.010
1.510,0.250
2.445,0.500
3.015,0.660
3.275,0.750

```
 3.495,0.845
 3.650,1.000
 3.715,1.095
 3.790,1.335
 3.795,1.500
 3.795,2.000
 3.795,2.500
 3.795,2.950
 3.795,3.000
 3.800,3.080
 3.000,3.080
 3.000,4.580
(midship section)
17,0.0
 0.000,0.000
 0.240,0.000
 0.250,0.015
 1.310,0.250
 2.455,0.500
 3.480,0.750
 3.655,0.925
 3.740,1.000
 3.795,1.205
 3.795,1.500
 3.795,2.000
 3.795,2.500
 3.795,2.995
 3.795,3.000
 3.800,3.074
 3.000,3.074
 3.000,4.574
(6 section)
18,3.45
```

0.000,0.120
0.240,0.120
0.240,0.140
0.810,0.250
1.925,0.500
3.005,0.750
3.355,0.900
3.525,1.000
3.665,1.245
3.750,1.500
3.800,1.815
3.795,2.000
3.795,2.500
3.795,2.995
3.795,3.000
3.800,3.074
3.000,3.074
3.000,4.574
(7 section)
19,6.90
0.000,0.235
0.245,0.235
0.245,0.245
0.275,0.250
1.410,0.500
2.430,0.750
2.780,0.900
3.000,1.000
3.230,1.255
3.430,1.500
3.580,1.900
3.625,2.000
3.690,2.320

3.735,2.500
3.795,3.000
3.795,3.060
3.800,3.074
3.000,3.074
3.000,4.574
(8 section)
19,10.35
0.000,0.360
0.240,0.360
0.240,0.370
0.915,0.500
1.395,0.655
1.670,0.750
1.995,0.945
2.145,1.000
2.495,1.350
2.650,1.500
2.800,1.795
2.955,2.000
3.120,2.395
3.200,2.500
3.310,2.860
3.390,3.000
3.450,3.120
3.000,3.120
3.000,4.620
(8+1/2 section)
18,12.075
0.000,0.410
0.235,0.410
0.235,0.420
0.655,0.500

0.990,0.650
1.230,0.750
1.470,0.925
1.615,1.000
1.845,1.280
2.055,1.500
2.220,1.805
2.370,2.000
2.505,2.310
2.645,2.500
2.755,2.820
2.880,3.000
2.990,3.190
2.990,4.690

(9 section)

19,13.80

0.000,0.485
0.240,0.485
0.240,0.500
0.340,0.500
0.615,0.650
0.800,0.750
0.955,0.910
1.065,1.000
1.240,1.300
1.360,1.500
1.505,1.845
1.600,2.000
1.725,2.345
1.825,2.500
1.935,2.800
2.080,3.000
2.410,3.620

```
 2.735,4.000
 3.730,5.190
(9+1/2 section)
18,15.525
 0.000,0.555
 0.175,0.555
 0.175,0.560
 0.405,0.750
 0.505,0.885
 0.590,1.000
 0.715,1.300
 0.795,1.500
 0.895,2.000
 0.960,2.500
 1.005,2.800
 1.120,3.000
 1.245,3.310
 1.520,3.735
 1.775,4.000
 2.010,4.365
 2.360,4.735
 3.150,5.290
(FP section)
18,17.25
 0.000,0.705
 0.065,0.705
 0.065,0.715
 0.095,0.750
 0.240,1.000
 0.360,1.285
 0.430,1.500
 0.455,1.815
 0.430,2.000
```

0.325,2.275
0.080,2.500
0.055,2.820
0.090,3.000
0.175,3.350
0.415,3.865
0.570,4.000
1.005,4.585
2.250,5.410

1

1